View metadata, citation and similar papers at core.ac.uk

brought to you by CORE

provided by Institutional Repository for Minnesota State University, Mankato

CORNERSTONE
Minnesota State University Mankato

Journal of Undergraduate Research at Minnesota State University, Mankato

Volume 17 Article 7

2017

Design and Validation of a Low Cost High Speed Atomic Force Microscope

Michael Ganzer
Minnesota State University, Mankato, michael.ganzer@mnsu.edu

Tien Pham
Minnesota State University, Mankato, tien.pham@mnsu.edu

Follow this and additional works at: http://cornerstone.lib.mnsu.edu/jur

Part of the Electrical and Electronics Commons, Nanoscience and Nanotechnology Commons, and the Signal Processing Commons

Recommended Citation

Ganzer, Michael and Pham, Tien (2017) "Design and Validation of a Low Cost High Speed Atomic Force Microscope," *Journal of Undergraduate Research at Minnesota State University, Mankato*: Vol. 17 , Article 7.
Available at: http://cornerstone.lib.mnsu.edu/jur/vol17/iss1/7

This Article is brought to you for free and open access by the Undergraduate Research Center at Cornerstone: A Collection of Scholarly and Creative Works for Minnesota State University, Mankato. It has been accepted for inclusion in Journal of Undergraduate Research at Minnesota State University, Mankato by an authorized editor of Cornerstone: A Collection of Scholarly and Creative Works for Minnesota State University, Mankato.

Student Agreement:
I am submitting my research article to be published in the JUR (The Journal of Undergraduate Research at Minnesota State University, Mankato), an electronic journal of the Minnesota State University Undergraduate Research Center.

I/We certify have followed the accepted standards of scientific, creative, and academic honesty and ethics.

I understand that my article submission will be blind-reviewed by faculty reviewers who will recommend acceptance for publication; acceptance with revisions; or reject for publication.

I understand that as author, I retain the right to present any part of the research in any form in other publications.

The JUR has the right to reproduce and reprint published submissions for instructional or promotional purposes.

For complete details, see *Journal of Undergraduate Research at Minnesota State University, Mankato policies page.*

Mentor Agreement:
I have reviewed the submission, and I support its inclusion in the JUR (The Journal of Undergraduate Research at Minnesota State University, Mankato). I understand that I will be acknowledged as the faculty mentor for the student author(s). To the best of my knowledge, the student has followed the accepted standards of scientific, creative, and academic honesty and ethics.

Design and Validation of a Low Cost High Speed Atomic Force Microscope

Student researchers: Michael Ganzer, Tien Pham; Faculty mentor: Dr. Robert Sleezer

8/14/2017

***Abstract*— The Atomic Force Microscope (AFM) is an important instrument in nanoscale topography, but it is expensive and slow. The authors designed an AFM to overcome both limitations. To do this, they used an Optical Pickup Unit (OPU) from a DVD player as the laser and photodetector system to minimize cost and they did not implement a vertical control loop, which maximized potential speed. Students will be able to be use this device to make nanoscale measurements and engage in micro-engineering. To prototype this idea, the authors tested an OPU with a silicon wafer and demonstrated the ability to consistently distinguish different distances based on the OPU output. Additional testing was done in order to measure the sensitivity of the OPU using a more robust signal conditioning system. The result of their work is that the system they designed has a resolution of 65 nm on static samples and 1 µm on dynamic samples. Further work is needed to improve the resolution of this system, reduce noise, calibrate the system, and minimize drift.**

---

1. INTRODUCTION

The Atomic Force Microscope (AFM) is an important tool in nanoscale material characterization which is used in many fields, including semiconductor design, medical research, and material science. It is used to get a topographical map of the surface of a material [1]. It can also be used to determine the 3D structure of molecules [2], measure particle velocity [3], and make current path maps of metals [4]. A diagram of an AFM is shown in Figure 1.

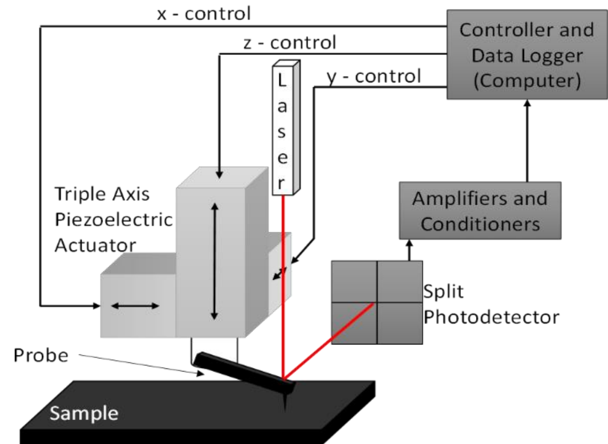

Figure 1. A basic diagram of the components in an AFM.

An AFM is controlled by a computer which sends control signals to a triple axis piezoelectric actuator. The piezoelectric actuator moves a cantilever with a probe on the end of it in three dimensions. The probe is sized for nanoscale measurements, with a typical probe diameter on the order of 10 nm. As the probe moves across a surface, the probe is deflected by changes in the surface elevation, causing a laser which is deflected off the cantilever to hit different locations on a photodetector. The signal from the photodetector is then conditioned and sent to the computer to interpret that data as an elevation and log the topographical data along the surface [5].

There are two primary disadvantages with most AFMs. The first disadvantage is that they are usually very expensive. An AFM generally costs around $250,000. One solution that has been used to mitigate this problem is using the optical pickup unit (OPU) of a CD or DVD player, which has been used as the laser and photodiode array system in an Atomic Force Microscope (AFM) [3], [6]-[11]. An OPU-based AFM can have a vertical resolution on the order of a nanometer [7] [8] [12], or even atomic resolution [9]. Because an OPU is

Published by Cornerstone: A Collection of Scholarly and Creative Works for Minnesota State University, Mankato, 2017

used in consumer electronics, it has been optimized for cost and is widely available. Figure 2 is a simplified circuit diagram of the OPU [13].

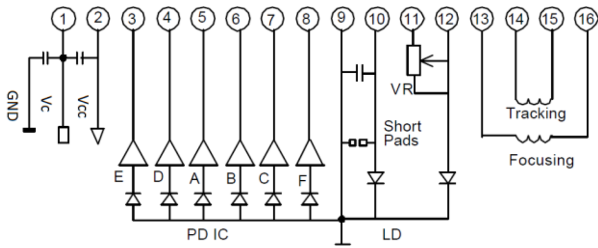

Figure 2. A basic diagram of the OPU circuit

The second drawback is that most AFMs have a slow imaging rate, making them suitable for only static samples. The reason for the slow measurement speed of most AFMs is that the computer controls them to maintain a constant deflection in the probe, using the control needed to determine the elevation of each point. This method of operation gives several advantages, including increased vertical range, higher precision, and not deforming soft samples [14]. However, it also limits the speed of the AFM. By turning off vertical control, the aforementioned advantages are lost but video rate imaging is possible.

Both disadvantages have been overcome individually, but not simultaneously in one device. Our goal is to make an AFM with a cost of approximately $1,000 and video rate (~30 fps) imaging. This paper details the results of our work adapting the KSS 213C OPU for use in the AFM.

a) OPU Pinout and Descriptions of Pins

The pinout of the KSS 213-C OPU used is shown in Table 1 [13].

Table 1: The pinout of the KSS 213-C OPU.

Pin	Function	Pin	Function
1	Vc	9	GND
2	Vcc	10	LD
3	E	11	Vref
4	D	12	PD
5	A	13	F+
6	B	14	T+
7	C	15	T-
8	F	16	F-

Pin 1 is the collector voltage and Pin 2 is the voltage beyond the collector voltage. These voltages are connected to the outputs of the photodiode array pins.

Pins 3 through 8 are the photodiode array pins. Pins 3 and 8 are connected to the tracking error, which is the radial positioning error. This error is a measure of how far outside the DVD grooves the laser is. For the application of an AFM, these pins will not be useful. Pins 4 through 7 are the focus error pins, which are a measure of the wobble of a DVD disk. For the AFM, they are the pins being used to measure the distance. The distance is linearly proportional to Equation 1

$$(A + C) - (B + D) \quad \textbf{Equation 1}$$

Pin 9 is the ground pin. Pin 10 is the laser diode pin. It powers the laser diode used to measure the distance. It requires at least 100 mA of current, but can go to at least 200 mA before burning out the laser diode.

Pin 11 is the reference voltage pin. It is somehow connected to reading the data from a disk. The documentation seems to indicate that it should be connected to ground, which doesn’t make much sense. Along with pin 12, which is also related to the data on a DVD disk, pin 11 is not used in the AFM circuit.

Pins 13 through 16 are control pins which control the position of the lens. 13 and 16 move the lens closer to and further from the disk. 14 and 15 move the lens closer to and further from the center of the disk in the radial direction. These pins were not

used in the AFM circuit, but could be powered to ensure stability of the lens position.

b) Constant Current Source

There are many methods of generating a constant current. One method is the current mirror. This circuit is shown in Figure 3.

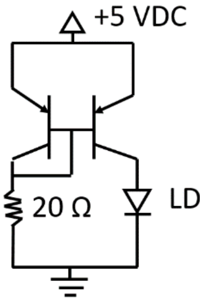

Figure 3. The PNP current mirror circuit.

There is a 0.7 V drop in voltage between the emitter and base of the PNP transistors. Because the base is jumpered to the collector of the reference (left one in the image) transistor, there is no voltage drop between those two pins. The voltage drop across the reference resistor must then be 4.3 V. Using the relationship between voltage, resistance, and current, the reference current can be found and is shown in Equation 2.

$$i = \frac{V}{R}$$ **Equation 2**

$$i_C = \beta i_B$$ **Equation 3**

Assuming that the beta parameter (described in Equation 3) of both transistors are the same value and that same value is infinity, then the current through the load (a laser diode in this case) should be equal to the current in the resistor.

Because the beta parameter of a transistor is not consistent between two of the same transistor model and because it is not infinite, that assumption is not true. Minor modifications need to be made to the reference resistor to ensure the correct current through the load. Another way to improve a current mirror is to use matched transistors, which come from the same batch in the factory, which allows them to have very similar values of the beta parameter.

Another issue which needs to be accounted for when using a current mirror is the load dependent nature of the load current. If the resistance of the load is in excess of the reference resistor, then the current through the load will be less than the reference current. Further alterations to the reference resistor can compensate for that issue.

c) Constant Voltage Source

There are many methods of generating a constant voltage source. One method of doing that is a voltage divider with a voltage follower. This circuit is shown in Figure 4.

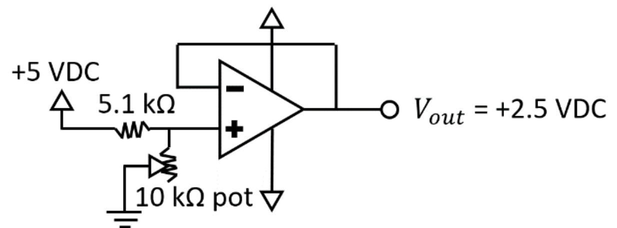

Figure 4. A diagram of a voltage divider with a voltage follower.

The voltage divider shown in this circuit uses a potentiometer to allow for quick adjustment of the output of the voltage divider, and thus the voltage source. The potentiometer should be calibrated such that the resistance from the op amp input to ground is approximately 5.1 kΩ. This makes the input voltage into the follower approximately 2.5 V.

The voltage follower is an op amp with a gain of 1. It acts as a buffer.

d) Capacitive Filtering of Power Supplies

To reduce the voltage ripple from a power supply, which is a high frequency noise element in the voltage from a supply, a capacitive filter can be placed between the source and ground in parallel with whatever loads are powered with the voltage supply. For low frequency components of overall

voltage, the capacitors act as an open circuit. For high frequency components of overall voltage (like voltage ripple), the capacitors act as a short circuit. This is depicted in Figure 5.

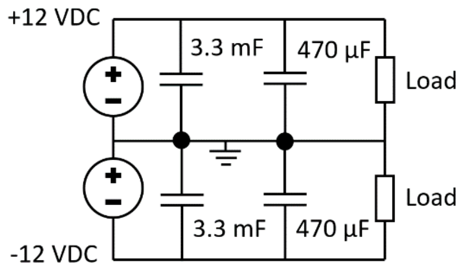

Figure 5. A circuit diagram of capacitive filtering of voltage ripple from voltage supplies.

e) Differential Amplification

To amplify the difference between two voltages, a differential amplifier made with an op amp is one method of doing that. This type of circuit is depicted in Figure 6.

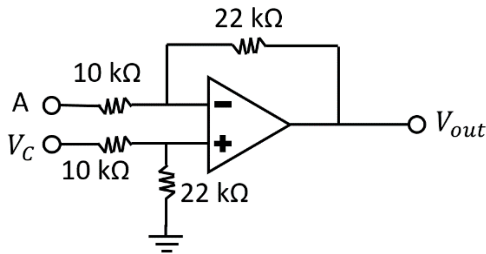

Figure 6. A circuit diagram of a differential amplifier.

Based on the op amp golden rules in Table 2 (which are a valid assumption if the output is connected to the inverting input), the output of this circuit as a function of the two inputs is Equation 4.

Table 2: The two golden rules of op amps with negative feedback.

1. The resistance between the inverting and noninverting input is infinitely large. Consequentially, no current will flow between those two inputs.
2. When there is negative feedback, the output will do whatever it can to make the inverting input and the noninverting input have the same voltage.

$$V_{out} = \frac{22\ k\Omega}{10\ k\Omega}(V_C - A) \qquad \textbf{Equation 4}$$

The gain is equal to the ratio of the feedback and ground resistors (22 kΩ) to the input resistors (10 kΩ).

f) Noninverting Amplifier

The same principles used to make a differential amplifier can also be used to make a noninverting amplifier. This is shown in Figure 7.

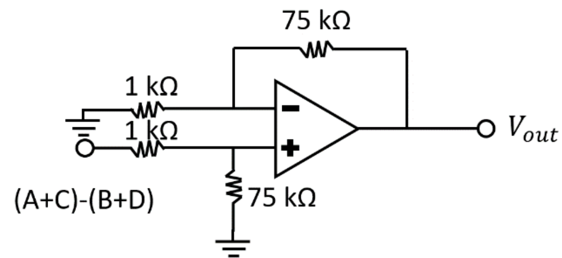

Figure 7. A noninverting amplifier.

As with the previous amplifier, the gain is equal to the ratio of the feedback and ground resistors (75 kΩ) to the input resistors (1 kΩ).

g) Summing Amplification

The summing amplifier is a op amp circuit which can add and subtract many inputs and amplify the resulting sum. This is shown in Figure 8.

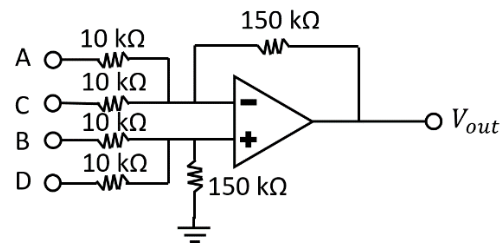

Figure 8. A summing amplifier.

The output of this circuit is shown in Equation 5.

$$V_{out} = \frac{150\ k\Omega}{10\ k\Omega}((B + D) - (A + C)) \qquad \textbf{Equation 5}$$

h) Nulling the Voltage Offset of an Op Amp

An ideal op amp will amplify the difference between the noninverting and inverting inputs. However, real op amps also have an input voltage offset which is amplified. Most op amps have pins which connect to an internal null offset circuit. However, those pins did not function as was specified in the spec sheet. Because of that discrepancy, other methods of null offsetting were investigated. One method is the circuit shown in Figure 9.

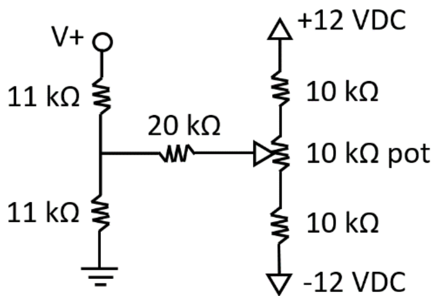

Figure 9. An external null offset circuit to be used with an op amp. V+ is the noninverting input.

By tuning the potentiometer, the voltage at the noninverting input can be altered to cancel out the effect of the input offset voltage.

2. METHODS

a) Initial Signal Conditioning

All the connection pins of the OPU and how they were operated are shown below (Figure 10). Pins 9 and 10 are used to power the laser diode while pins 1 and 2 power the photoarray. The output pins of the photoarray are 4,5,6 and 7 and are connected to non-inverting amplifiers.

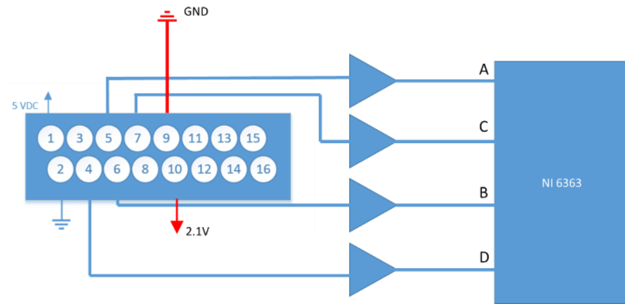

Figure 10. The laser diode power connection is shown in red. (Pin 9 and 10). Photo array power connection is shown in blue (pin 1 and 2). The A, B, C, and D element of the Photo array is amplified and connected to the NI6363 DAQ as for inputs to the LabVIEW

LM741 operational amplifiers were used to amplify each output pin of the OPU. The gain of each amplifier was about 20dB. The output pin of each amplifier was connected to ground with a 10k resistor to prevent floating current.

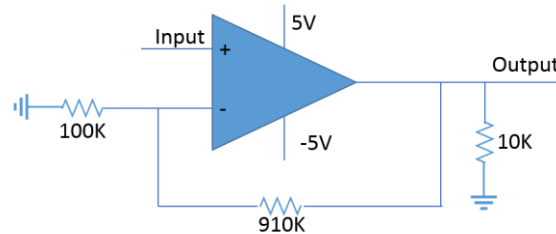

Figure 11. The non-inverting amplifier circuit used to amplify signal from the OPU to the input signals of LabVIEW

A LabVIEW program was used to acquire the four amplified signals from the OPU in the time and frequency domain. The program is shown in Figure 12.

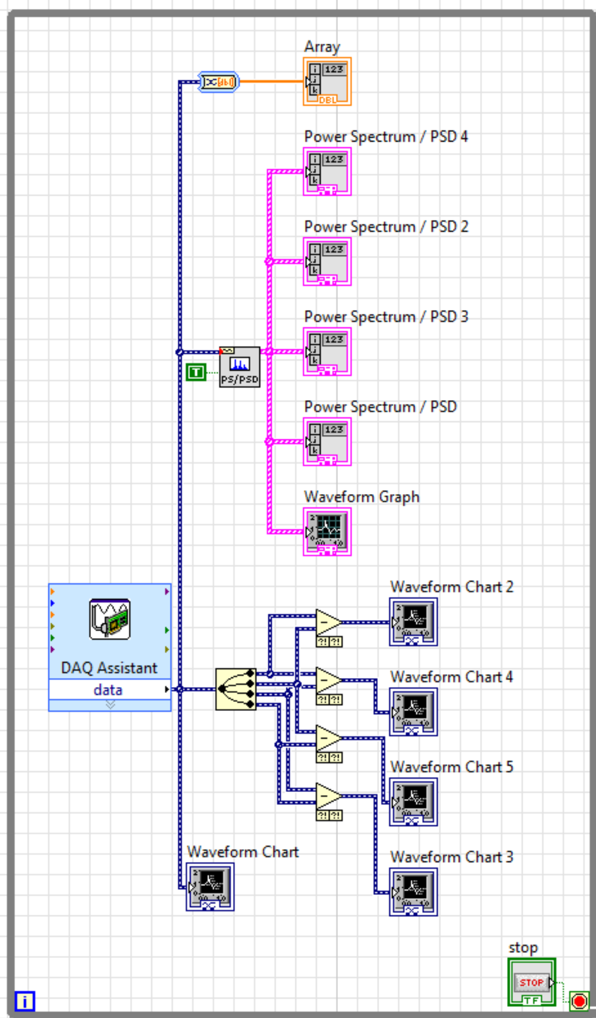

Figure 12 The LabVIEW program with the signal in time domain and also frequency domain. The differential signals were also used to examine its change when there is change in the input signals

b) First Testing Apparatus

The initial testing apparatus is shown in Figure 13. The lead screw and OPU laser beam are in line with each other. The silicon wafer disk is attached to the lead screw so that the laser beam is perpendicular to the silicon surface. The lead screw can move back and forth so that the silicon can be moved relative to the OPU. The angle indicator shown in Figure 14 was used to indicate the rotational position of the silicon wafer compared to the OPU position, which, with the pitch of the leadscrew, can be related to the distance between the OPU and the wafer. The silicon wafer was turned to three different angular positions (210º, 220º, and 240º) and the average voltage of each OPU output pin and the DC offset of each pin was recorded for each angle.

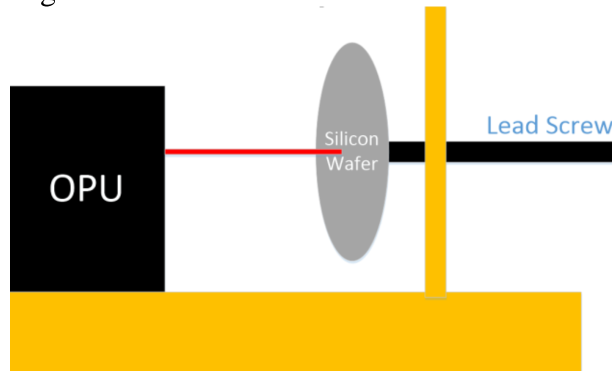

Figure 13. The testing apparatus used to calibrate the output signal of the OPU. There is an angle indicator attached to the silicon wafer to measure the rotational movement of the lead screw

Figure 14. The angle indicator shown on the right view side of the testing apparatus. The three positions used to measure the electrical signal response were 210, 220 and 240 degrees.

c) Static Measurement Testing

An iterated AFM apparatus was built (Figure 15). The 2 cross bars that attach the OPU can be freely moved by adjusting the screw which is screwed in the cross bar and placed on the top of the right block. The silicon wafer is placed statically on the base of the design.

The original signal of the OPU was recorded when there is no weight applied to the top of the screw. Two different weights (2 lbs and 5 lbs) were placed on the top of the nail one after another while the data measured by the OPU was being recorded. The change in height of the screw is also the change in the distance between the OPU and the silicon wafer with the change in horizontal distance was neglected as the angle deflection is relatively small.

Using stress and strain analysis, the strain of the screw was measured based on different weight applied. Relationship between stress (σ) and strain (ϵ) are shown in **Equation 6** with Young's modulus E, which is a property of the material that makes up the screw. The input parameter of the screw can be seen in Table 3.

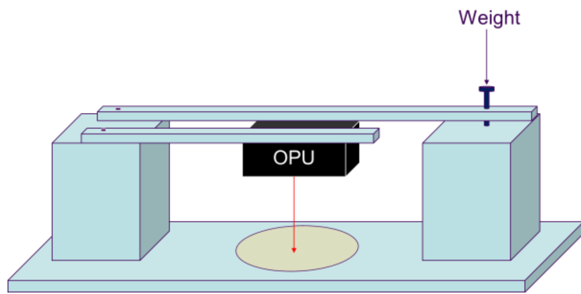

Figure 15. Second iteration of the AFM design

$$\sigma = E\epsilon \qquad \textbf{Equation 6}$$

Table 3 input parameters of the screw

Young's modulus (Pa)	$2.0e + 11$
Cross diameter (inch)	0.0635
Original length (mm)	3.000

d) Modified Circuit

After the initial testing and static testing, the signal conditioning and OPU power circuitry were modified in an attempt to improve resolution.

The OPU was operated as described in Table 4. All other pins were not connected.

Table 4: The OPU operation parameters used in this experiment.

Pin Number	Pin Function	Pin Type
1	Vc (2.5 VDC)	Voltage Input
2	Vcc (5 VDC)	Voltage Input
4	D	Voltage Output
5	A	Voltage Output
6	B	Voltage Output
7	C	Voltage Output
9	GND	Voltage Input
10	Laser Diode (~200 mA)	Current Input

Figure 3 (the PNP current mirror) was used to provide the current to the Laser Diode pin of the OPU (Pin 10).

Figure 4 (the voltage source) was used to provide the 2.5 V to Vc on the OPU (Pin 1). The op amp for this voltage source was a LM741 op amp. All op amp rails in this circuit are +12 VDC and -12 VDC.

Professionally manufactured voltage regulators were used for the +12 VDC, -12 VDC, and +5 VDC voltage supplies. Figure 5 (the capacitive filtering) was used to filter the +12 VDC and -12 VDC power supplies. The +5 VDC and +2.5 VDC power supplies did not have capacitive filtering on them.

Figure 6 (the differential amplifier) was used as the first stage of amplification. All amplification circuit op amps are the TL084CN low noise op amp. The gain is 2.2. Each of the four photodiode segments (A, B, C, D) was connected to the inverting input of a separate differential amplifier and Vc (Pin 1 of the OPU) was connected to the noninverting input of each of the differential amplifiers. Together, those four differential amplifiers are the first stage of the amplification.

Figure 7 (the noninverting amplifier) is the third stage of amplification. The output from the second stage is the noninverting input. The gain is 75. The output from the third stage was sent into a DAQ, into LabVIEW to be further processed.

Figure 8 (the summing amplifier) is the second stage of amplification. The outputs from the first stage are the inputs to the second stage. The gain of the second stage is 15.

Figure 9 (the external null offset) was not used in the final version of this circuit.

e) Dynamic Measurement Testing

This circuit was built on a breadboard and used with the OPU to find the distance between the OPU and an oscillating piezoelectric device. The piezoelectric device's oscillation frequency is 1 Hz in every trial. Voltages of 20 Vpp, 10 Vpp, 5 Vpp, 2.5 Vpp, 1 Vpp were used to excite the piezoelectric. Both sinusoidal and square waves were used. The test apparatus is shown in Figure 16. By using a profilometer, we found that the deflection of the piezoelectric material we used was approximately 250 nm/V.

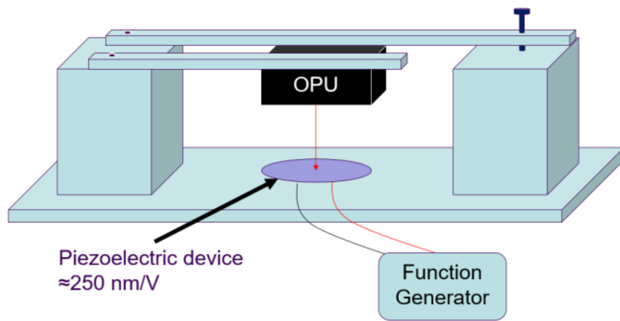

Figure 16. The piezoelectric testing schematic.

When the voltage was put into the DAQ, software-based filtering in LabVIEW was applied. The software filter was a third order low pass Butterworth filter with a cutoff frequency of 10 Hz.

3. RESULTS

a) Initial Test Apparatus Results

Figure 17 is a graph of the DC offsets of the four focus voltages of the OPU for each angle tested. Figure 18 is a graph of the average voltage of the four pins for each angle tested.

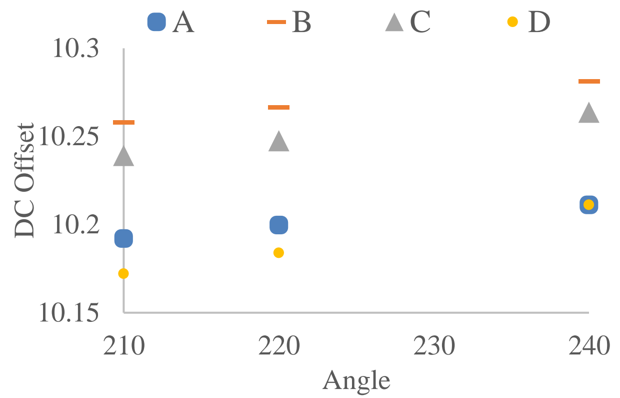

Figure 17. DC offset measurement from LabVIEW at 3 different position of the lead screw compared to the silicon wafer

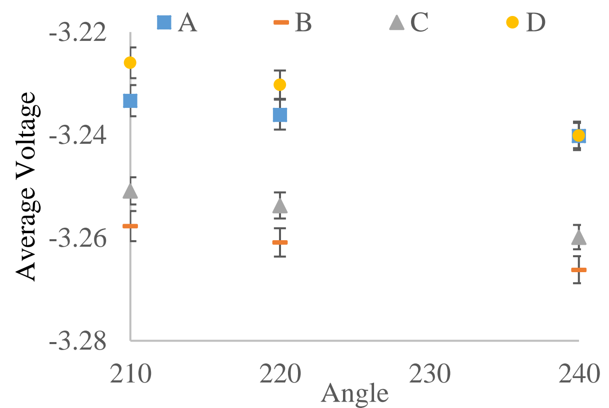

Figure 18. The average voltage signals over time of the three different positions of the lead screw over time

b) Static Test Results

The static test results are shown in Figure 19 with the change in height of the screw corresponding to the change in output signals of the OPU.

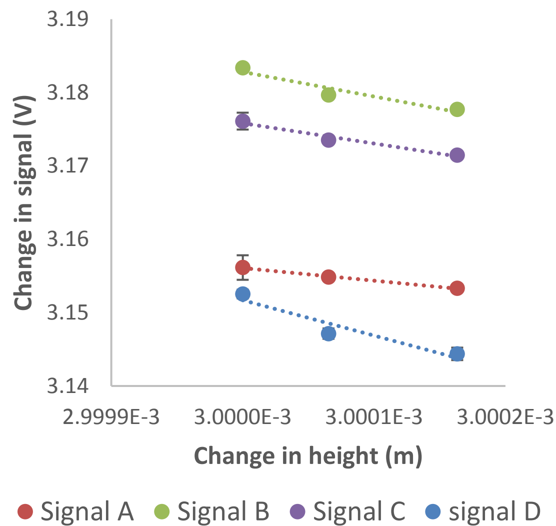

Figure 19. Static test results of the four output pins A, B, C, and D resulting from the static testing apparatus having different forces applied to it.

c) Dynamic Test Results

The results from the sinusoidal excitation tests are shown in Figure 20.

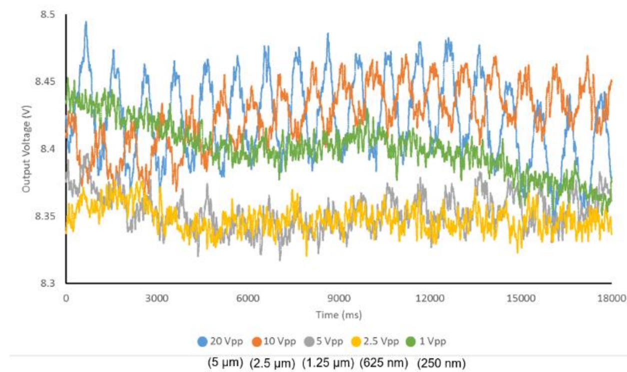

Figure 20. Results of tests with sinusoidal excitation of the piezoelectric material.

The results from the square wave excitation tests are shown in Figure 21.

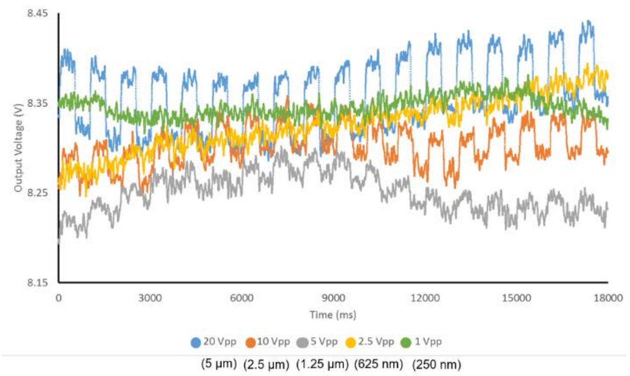

Figure 21. Results of tests with square wave excitation of the piezoelectric material.

The Laplace transform was used to turn time domain result data into frequency domain data. The frequency domain data from the 1 Vpp tests (sinusoidal and square wave) is shown in Figure 22.

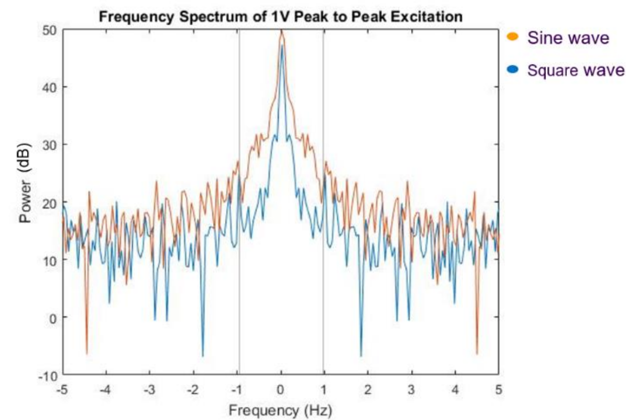

Figure 22. Frequency domain data from the sinusoidal and square wave tests with amplitude of 1 Vpp. The vertical lines designate the location of 1 Hz.

4. DISCUSSION

From this experiment and the results, it can be shown that the OPU system is able to consistently distinguish different distances qualitatively. However, the error of the measurements is such that that cannot be said with 95% confidence. The authors believe that with proper control of the focus and tracking controls of the OPU, a method of amplifying the OPU outputs further, and a more precise method of driving the sample, the noise level will be reduced and the OPU will exhibit greater resolution.

The static test results show a linear relationship between the measured distance and the 4 output signals of the OPU even though the linear constant are not the same across these 4 output pins. The resolution found of the device in this test is 65nm which is approach the requirement for the nanoscale measurement device.

In the dynamic tests, for higher excitation values, the peaks and valleys of the data are more apparent. However, for the lower excitation values, the peaks and valleys are not distinguishable from the noise of the system and the drifting of the voltage over time. Voltage drift can be caused by an OPU. This voltage drift results in measurement drift up to the micron range. However, drift caused by an OPU can be mitigated by utilizing the OPU's focus lens actuation. [10]

Based on the time domain data, the OPU has a resolution of approximately 1 μm when measuring a moving object. However, the frequency domain data seems to indicate a higher magnitude at 1 Hz (the piezoelectric material oscillation) than at higher frequencies (noise). It is presently uncertain if this difference in magnitude is significant or not. Further improvements to this circuit and additional testing will give a clearer idea of the significance or lack thereof of the 1 Vpp results. If they are significant, then this circuit has a resolution of at least 250 nm, if not better, when measuring moving objects.

To resolve these issues, better op amps should be put into this circuit, which should be put on a PCB. Chopper op amps, which are designed to minimize drifting, are recommended. However, the drift might also be a result of the amplification circuit topology as well as the op amps themselves. Additionally, external null offsets should be implemented.

Other elements will need to be put into the circuitry of the AFM eventually. One of those elements is a piezoelectric sample stage to move the sample in the horizontal directions. A control signal could be sent from LabVIEW into an audio amplifier, a device designed to have great linearity, to be amplified and sent to the piezoelectric sample stage, which requires high voltage.

Another additional element is focus and tracking control on the OPU lens. Controlling these elements could result in greater resistance to vibrational disturbances, which could reduce errors in the readings.

Earlier in the project, hardware-based filtering of high frequency noise in the photodiode output voltages was attempted, but this made the amplifiers almost unstable and resulted in a much greater drift than what is seen in the results. However, software based filtering does not have these issues.

To complete the AFM, the authors will need to find a way to increase the resolution of the readings, write a program to automate it, tune the control system, and calibrate the AFM with known samples.

5. CONCLUSION

The results of the experiments are promising, and further improvements to the AFM will result in improved resolution nearly comparable to commercial AFMs and a system which can be used by students for nanoscale measurements and design. Using op amps which are better optimized for small signal instrumentation, implementing the circuit on a PCB, adding external null offsets, a piezoelectric sample stage, and focus and tracking control could all improve the resolution of this AFM.

6. REFERENCES

[1] G. Binnig and C. F. Quate, "Atomic Force Microscope," *Physical Review Letters,* vol. 56, no. 9, pp. 930-933, 1986.

[2] C. Moreno, O. Stetsovych, T. K. Shimizu and O. Custance, "Imaging Three-Dimensional Surface Objects with Submolecular Resolution by Atomic Force Microscopy," *Nano Letters,* vol. 15, pp. 2257-2262, 2015.

[3] F. Quercioli, A. Mannoni and B. Tiribilli, "Laser Doppler velocimetry with a compact disc pickup," *Applied Optics,* vol. 37, no. 25, pp. 5932-5937, 1998.

[4] C. Rodenbücher, G. Bihlmayer, W. Speier, J. Kubacki, M. Wojtyniak, M. Rogala, D. Wrana, F. Krok and K. Szot, "Detection of confined current paths on oxide surfaces by local-conductivity atomic force microscopy with atomic resolution," 2016.

[5] S. Alexander, L. Hellemans, O. Marti, J. Schneir, V. Elings, P. K. Hansma, M. Longmire and J. Gurley, "An atomic-resolution atomic-force microscope implemented using an optical lever," *Journal of Applied Physics,* vol. 65, no. 1, p. 164, 1989.

[6] T. Corlson, "High Speed Atomic Force Microscope Design Using DVD Optics," Virginia Commonwealth University, 2014.

[7] J. Cui, X. Bian, Z. He, L. Li and T. Sun, "A 3D nano-resolution scanning probe for measurement of small structures with high aspect ratio," *Sensors and Actuators A: Physical,* vol. 235, pp. 187-193, 2015.

[8] K. Ehrmann, A. Ho and K. Schindhelm, "A 3D optical profilometer using a compact disc reading head," *Meas. Sci. Technol.,* vol. 1998, no. 9, pp. 1259-1265, 1998.

[9] E.-T. Hwu, K.-Y. Huang, S.-K. Hung and I.-S. Hwang, "Measurement of Cantilever Displacement Using a Compact Disk/Digital Versatile Disk Pickup Head," *Japanese Journal of Applied Physics,* vol. 45, no. 38, pp. 2368-2371, 2006.

[10] E.-T. Hwu, H. Illers, W.-M. Wang, I.-S. Hwang, L. Jusko and H.-U. Danzebrink, "Anti-drift and auto-alignment mechanism for an astigmatic atomic force microscope system based on a digital versatile disk optical head," *Review of Scientific Instruments,* vol. 83, no. 13703, 2012.

[11] W.-M. Wang, C.-H. Cheng, G. Molnar, I.-S. Hwang, K.-Y. Huang, H.-U. Danzebrink and a. E.-T. Hwu, "Optical imaging module for astigmatic detection system," *Review of Scientific Instruments,* vol. 87, no. 53706, 2016.

[12] T. Kohno, N. Ozawa, K. Miyamoto and T. Musha, "High precision optical surface sensor," *Applied Optics,* vol. 27, no. 1, pp. 103-108, 1988.

[13] LTD, Smartech Electronics and Machinery Manufacturing Co., "CD/VCD PICKUP SPECIFICATIONS MODEL:KSS-213C(FOR KSM-213CCM)," LTD, Smartech Electronics and Machinery Manufacturing Co., [Online]. Available: http://www.farnell.com/datasheets/1944121.pdf.

[14] G. Schitter and M. J. Rost, "Scanning probe microscopy at video-rate," *Materials Today,* vol. 11, pp. 40-48, 2008.

Published by Cornerstone: A Collection of Scholarly and Creative Works for Minnesota State University, Mankato, 2017